HHS Public Access

Author manuscript

J Mol Neurosci. Author manuscript; available in PMC 2020 August 01.

Published in final edited form as:

J Mol Neurosci. 2019 August ; 68(4): 603–619. doi:10.1007/s12031-019-01321-z.

Knockdown siRNA Targeting the Mitochondrial Sodium-Calcium Exchanger-1 Inhibits the Protective Effects of Two Cannabinoids Against Acute Paclitaxel Toxicity

Douglas E. Brenneman[1,2], **William A. Kinney**[2], and **Sara Jane Ward**[3]

[1]Advanced Neural Dynamics, Inc, Pennsylvania Biotechnology Center, Doylestown, PA 18902

[2]Kannalife Sciences, Inc, Pennsylvania Biotechnology Center, Doylestown, PA 18902

[3]Center for Substance Abuse Research, Department of Pharmacology, Lewis Katz School of Medicine, Temple University, Philadelphia, PA 19140

Abstract

Treatment with cannabidiol (CBD) or KLS-13019 (novel CBD analogue), has been shown previously to prevent paclitaxel-induced mechanical allodynia in a mouse model of chemotherapy-induced peripheral neuropathy (CIPN). The mechanism of action for CBD- and KLS-13019-mediated protection now has been explored with dissociated dorsal root ganglion (DRG) cultures using siRNA to the mitochondrial Na^+ Ca^{2+} exchanger-1 (mNCX-1). Treatment with this siRNA produced a 50–55% decrease in the immunoreactive (IR) area for mNCX-1 in neuronal cell bodies and a 72–80% decrease in neuritic IR area as determined with high content image analysis. After treatment with 100 nM KLS-13019 and siRNA, DRG cultures exhibited a 75 ± 5 % decrease in protection from paclitaxel-induced toxicity; whereas siRNA studies with 10 μM CBD produced a 74 ± 3% decrease in protection. Treatment with mNCX-1 siRNA alone did not produce toxicity. The protective action of cannabidiol and KLS-13019 against paclitaxel-induced toxicity during a five hour test period was significantly attenuated after a four day knockdown of mNCX-1 that was not attributable to toxicity. These data indicate that decreases in neuritic mNCX-1 corresponded closely with decreased protection after siRNA treatment. Pharmacological blockade of mNCX-1 with CGP-37157 produced complete inhibition of cannabinoid-mediated protection from paclitaxel in DRG cultures, supporting the observed siRNA effects on mechanism.

Keywords

sodium-calcium exchanger -1 (NCX-1); chemotherapy; paclitaxel; cannabidiol; siRNA; dorsal root ganglion

Corresponding author: Douglas E. Brenneman, Ph.D., Advanced Neural Dynamics, Inc, Pennsylvania Biotechnology Center, 3805 Old Easton Road, Doylestown, PA 18902, Ph: 1-215-589-6317, FAX: 215-589-6335, dbrenneman@advneuraldynamics.com.

Introduction

The medical uses of cannabis and the non-psychotropic cannabis component cannabidiol (CBD) have attracted significant public interest for compassionate treatment of diseases that currently are refractory to conventional therapies (Lim et al, 2017). Among the unmet medical needs that cannabis and cannabidiol have been purported to have is in pain management (Darkovska-Serafimovska et al., 2018). Of particular therapeutic interest now was the potential of CBD in the treatment of chemotherapy-induced peripheral neuropathy (CIPN), a painful adverse effect caused by several classes of widely used anticancer drugs (Seretny et al., 2014). Symptoms of CIPN are typically peripheral and sensory in nature, consisting of mechanical, heat and cold hypersensitivities with ongoing burning pain, tingling and numbness. Currently, there is no one drug or drug class that is considered both effective and safe in the treatment of CIPN. In many cases, this neuropathic pain associated with CIPN can result in a dose-limiting side effect which, in severe cases, can progress to an irreversible condition (Argyriou et al., 2014).

In a mouse model of CIPN that focused on paclitaxel-induced mechanical and cold allodynia, CBD was observed previously to be effective in preventing the onset of this treatment consequence (Ward et al, 2011; 2014; King et al., 2017). Importantly, a new CBD analogue (KLS-13019) has been synthesized that has improved drug-like properties in comparison to CBD, while retaining neuroprotective properties. In preliminary studies, a significant preventative action on paclitaxel-induced mechanical allodynia in a mouse model of CIPN also has been reported for KLS-13019 (Ward et al., 2017).

In contrast to the limited knowledge of KLS-13019 pharmacology, the reported molecular targets of CBD for neurological disorders alone are extraordinarily numerous (Bih et al., 2015). Focusing only on those targets relevant to overlapping actions between the two cannabinoids, our mechanistic goal was to explore mNCX-1 as a molecular target of the actions for protection from paclitaxel in CIPN. The rationale for exploring mNCX-1 as a target resided in three areas of previous research. Initially, our interest in mNCX-1 was based on the observations that CBD targeted the mitochondria of hippocampal neurons to regulate intracellular calcium concentrations (Ryan et al., 2009). Related studies confirmed that a primary function of mNCX-1 was to regulate calcium levels by extruding calcium into the cytosolic compartment (Palty et al., 2010), although this exchanger can also function in a reverse mode to take up calcium (Blaustein and Lederer, 1999). Because of the critical importance of calcium homeostasis in maintaining neuronal viability (Celsi et al., 2009), mNCX-1 was concluded to be of fundamental importance in preventing cellular damage and death associated with calcium dysregulation. Secondly, previous studies indicated that abnormalities in calcium signaling and increased reactive oxygen species (ROS) occurred as a result of mitochondrial dysfunction in CIPN (Canta et al., 2017). Relevant to the current studies, among the toxic properties of paclitaxel was an increase in ROS (Duggett et al., 2016) that was only evident in a subpopulation (non-peptidergic) of DRG neurons that were positive for isolectin-B4. In preliminary experiments, we also have observed increased fluorescence with ROS-sensitive dyes after acute (3 hours) treatment of DRG cultures with 3 μM paclitaxel. Lastly and arguably the most pertinent and compelling evidence of mNCX-1 involvement as a cannabinoid mechanism is the observed pharmacological prevention of the

protective actions of KLS-13019 and CBD in hippocampal cultures (Brenneman et al., 2017). These recent studies have shown that cannabinoid-mediated neuroprotection from oxidative stress-related toxicities was completely blocked by the CGP-37157, specific inhibitor of the mitochondrial $Na^{+}Ca^{+2}$ exchanger-1 (mNCX-1).

The protective properties of KSL-13019 and CBD in preventing paclitaxel- induced toxicity now have been explored with small interfering RNA (siRNA) to the mNCX-1 target in dorsal root ganglion (DRG) cultures. This cellular strategy was based on the recognition that sensory neurons residing in DRG are a primary mediator of CIPN (Argyriou et al., 2014). The use of siRNA to produce a partial depletion of mNCX-1 target as a means of further exploring the relationship between these cannabinoids and this complex mitochondrial target was chosen because the complete deletion of mNCX-1 resulted in embryonic lethality (Cho et al., 2003). While siRNA knockdown strategies typically use mRNA levels, target immunoreactivity measures from a Western blot analysis or biological loss of function as a means of assessing target depletion, the present studied employed a combination of methodologies. In the studies to be reported, high content fluorescent imaging of DRG neurons were used to assess target depletion in this model system that is relevant to CIPN (Guo et al., 2017). With the utilization of this imaging technique applied to the diversity and complexity inherent to primary sensory neuron morphology, the goal was to compare the neuronal depletion of mNCX-1 target and the reduction of protective activity produced by the two cannabinoids from paclitaxel-induced toxicity. Importantly, by utilizing the capability of high content imaging, the feasibility of distinguishing and comparing the responses of neurites and cell bodies of sensory neurons in regard to mNCX-1 immunoreactivity was realized.

The specific aim of the present study was to assess the effect of mNCX-1 knockdown in preventing the protective actions of two cannabinoids against acute paclitaxel-induced toxicity in dorsal root ganglion cultures. The choice of utilizing a relatively short treatment period was two-fold: 1) to focus only on an initial phase of reproducible paclitaxel toxicity to determine if the target knockdown mNCX-1 prevented the acute cannabinoid-mediated protection; and 2) to focus only on early events in paclitaxel toxicity thus decreasing the probability of involvement of longer term responses such as changes in axonal transport and gene expression which add more mechanistic complexities.

Materials and Methods

Materials

The following reagents were obtained from Sigma-Millipore (St Louis, MO): 6-carboxyfluoresceine diacetate (CFDA, C5041); dimethyl sulfoxide (472301); 7-Chloro-5-(2-chlorophenyl)-1,5-dihydro-4,1-benzothiazepin-2(3H)-one (CGP-37157; C8874). Alamar Blue (DAL 1025) and nerve growth factor (13290010) were obtained from Invitrogen (Eugene, Or). Paclitaxel was obtained from Teva Pharmaceuticals USA (Sellersville, PA) as a 6 mg/ml solution containing 527 mg polyoxyl 35 castor oil, 2mg citric acid and 49.7% dehydrated alcohol /ml. The synthesis of KLS-13019 has been described previously in detail (Kinney et al., 2016). Verification of the structural identity for KLS-13019 was determined by ^{1}H NMR, LC/UV, and LC/MS. The purity of KLS-13019 was 98.6% as determined by

LC/MS. For the siRNA directed to the mitochondrial Na^+ Ca^{2+} exchanger (mNCX-1) target (Rat Slc8b1), a pool of 4 oligonucleotides was utilized from Dharmacon (Lafayette, CO). The target siRNA sequences were as follows: 1) CGACAAGGAUGAUCGGAAC; 2) GGGCUGUAGUGGUGAUCGU; 3) GUGGAGAACUCAGUCGAUA; and 4) UACCAAAGGCAGCGGAGCA. In addition, a non-targeting control siRNA was also tested with the following structure: UGGUUUACAUGUCGACUAA.

Culture model

Dissociated dorsal root ganglia (DRG) cultures derived from embryonic day 18 rats were employed as the primary assay system to explore mechanism of action studies for cannabidiol and KLS-13019-mediated protection. In brief, DRG were obtained commercially through Brain Bits (Springfield, IL) and cultures prepared with slight modifications to methods previously described (Brewer et al., 1993). Tissue was dissociated with a papain-based kit from Worthington Biochemical Corporation (Lakewood, NJ). The DRG cells were plated at low density (10,000 cells / well) in a 96-well format and maintained in serum-free medium consisting of Neurobasal Medium supplemented with B27, GlutaMAX (Gibco) and 25 ng/ml Nerve Growth Factor. Poly-D-lysine coated plates (BD Biosciences, Franklin Lakes, NJ) were employed for this culture system. Prior to the initiation of experiments between days 5 and 9 in vitro, a complete change of medium was performed in a working volume of 100 μL.

mNCX-1 knockdown

Using the ON-targetplus SMARTpool siRNA described above, the pool of oligonucleotides were added to the cultures after a complete change from nutrient medium to 100 μl of Accell siRNA delivery medium (B-005000–500 from Dharmacon; Lafayette, CO). Preliminary experiments were conducted to determine that 100 nM to 1 μM of the siRNA produced the maximal amount of decrease in the immunoreactive area for the mNCX-1 target in neurons as determined by high content image analysis by methods to be described. For all experiments, 1 μM siRNA was used to decrease the mNCX-1 target in the DRG cultures. The progressive sequence of the siRNA treatment and response periods are shown in Figure 1. NGF (25 ng/ml) was added to the delivery medium during the 24 hour transfection period starting on day 5 after plating. After the siRNA treatment, a complete change of medium was performed to the serum-free nutrient medium containing NGF for an additional 4 days to allow time for further target silencing. Preliminary experiments were performed after the 24 hour transfection procedure to demonstrate that no toxicity was evident by the two cell viability assays employed for these studies. These same viability assays, along with image analysis of 7 neuronal parameters, were conducted on day 9 after the final mNCX-1 knockdown period.

Immunocytochemistry assays

To assess the effects of the siRNA treatment, immunocytochemical methods were used to measure neuronal, mitochondrial and mNCX-1 responses in the DRG cultures. The goals for these assays included: 1) to assess the immunoreactive knockdown of the mNCX-1 target with two different antibodies; 2) to compare the responses of both neuronal cell bodies and

neurites; and 3) to compare the responses of mNCX-1 immunoreactive area with that of a mitochondrial marker: cytochrome c oxidase 4 (COX4).

Prior to fixation, growth medium was removed and the wells were rinsed one time with 37° C DPBS. This warm rinse is particularly important to maintain structural stability of neurites. After removal of the DPBS, cultures were fixed for 20 min at room temperature with 50 μL / well of 3.5% formaldehyde (Sigma-Aldrich: 252549) in warm (37°C) DPBS that contained 5.5 μg/mL of Hoechst 33342 dye (Invitrogen: H3570) to label cell nuclei. After removal of the fixative, the cultures were rinsed twice with 100 μL of DPBS and then a permeabilization/ blocking buffer containing 5% normal goat serum and 0.3% triton-X100 in DPBS was added to the cultures for 10 min. After removal of the blocking buffer, the cultures were rinsed twice with 100 μL of DPBS and then primary antibodies were added for one hour incubation at room temperature. Two antibodies were used to compare changes in mNCX-1 immunoreactive responses. The first antibody used to detect mNCX-1 was AB3516P, a rabbit antiserum that was made against a 23 amino acid peptide sequence from the cytoplasmic domain 3 of rat NCX-1 (Millipore). This antiserum was used at 1:300 with a secondary antibody of goat anti-rabbit labeled with Alexa Fluor 568 (A-11011 (Life Technologies) used at 1:2000. The second anti-mNCX-1 was C2C12, a mouse monoclonal antibody made against purified canine cardiac sodium-calcium exchanger-1 (Novus Biologicals, Centennial, CO). C2C12 was used at 1:400, with a secondary antibody of goat anti-mouse labeled with Alexa Fluor 647 (A-21235, Life Technologies) used at 1:2000. Both these antibodies to mNCX-1 resulted in similar results after image analysis of immunoreactive spot areas on neurons. Because of this similarity in the response to these primary antibodies, the AB3516P antibody was used throughout these studies. The primary antibody used as a marker for mitochondria was GT6310 for cytochrome c oxidase 4 (Life Technologies). GT6310, used at 1:300, is a mouse monoclonal antibody that was made to a recombinant fragment between amino acid 1–169 in COX4. The secondary antibody (A-21037) for the COX4 assay was goat anti-mouse labeled with Alexa Fluor 750 (Life Technologies) that was used at 1:1000. Neurons were identified with antiserum to type III beta tubulin (tuj 1) to measure changes in all neuronal parameters. The primary antiserum employed was rabbit anti-human obtained from Sigma –Aldrich (T2200) and used at 1:400 dilution. The secondary was an Alexa Fluor 488-conjugated Fab fragment of goat anti-rabbit IgG obtained from Life Technologies (A11070) used at 1:600. With all assays after the secondary antibody treatment, cultures were rinsed 3 times with 100 μL of DPBS before performing high content fluorescent analysis. For storage, the wells were placed in 100 μL of sterile DPBS, with the plates wrapped in aluminum foil and maintained at 4° C.

High content image analysis—The immunocytochemical assays were conducted on the Cell Insight CX5 high content imaging system (Thermo Fisher Scientific). The system is based on an inverted microscope that automatically focuses and scans fields of individual culture wells using a motorized stage at predetermined field locations. Fluorescent images from individual fields (895μm × 895μm) were obtained with a 10 × (0.30NA) Olympus objective and Photometrics X1 CCD camera, with analysis by HCS Studio 2.0 Software. The light source was LED with solid state five-color light engine used with filter sets that had the following excitation/emission: 386/440, 485/521, 560/607, 650/694 and 740/809).

With this capability, multiple fluorescent assays in a single well were conducted. Images were acquired in a low resolution mode (4 × 4 binning). Image analyses for neuronal cell bodies and neurites were performed with the Cellomics Neuronal Profiling BioApplication. For analysis of neurons, objects were identified as cells if they had valid nuclei and cell body measures based on size, shape and average intensity. Acceptable ranges were determined in preliminary studies to ensure that aggregated cells and non-cellular objects were excluded from the analysis.

Because most mitochondria are localized in the cell bodies of DRG neurons, the initial type of image analyses were focused on mNCX-1 and COX4 (mitochondrial marker) immunoreactive spots using the Cellomics General Spot Analysis Measurement Tool BioApplication. This algorithm was performed to measure the siRNA-induced changes in the cytoplasmic region of all cells. This general analysis of immunoreactive spots was defined by three imaging parameters: 1) the cellular localization of the spots; 2) the size of the spots; and 3) the threshold of pixel intensity of the spots that determined objects of interest from background. As the first measure for spot analysis for immunoreactive spot area in all cells, a “ring-spot” analysis was performed to confine and define the assay to a “region of interest” which excluded the nuclear domain (12 μm in width) as guided by the fluorescent area identified with the Hoechst 33342 dye, but included spots within a ring area that was 18μm in width. With this analysis, the spots appearing in neurites that extended beyond this “region of interest” were not included by this method, but the ring-spot domains from all cells comprised these analyses, including non-neuronal cells that were sparse (<10–20% of all cells) in number, but present in the DRG cultures. Because the ring-spot analysis is confined to the cytoplasmic region of each cell, this analysis provided the first assessment and point of comparison for the spot analysis. However, because the observed percentage loss (55 %) of immunoreactive mNCX-1 spot area was significantly less than the percentage loss (75%) of CBD-mediated protection from paclitaxel, another type of image analysis for mNCX-1 was also employed to extend the comparisons to the entire neuron: spot analysis embedded in the neuronal profiling bioapplication to permit an analysis of target loss from different neuronal regions.

For a follow-up type of the analysis of the same cultures, the goal was to examine the spot area of mNCX-1 only in the neurons of the DRG cultures, with a goal of comparing the cell bodies and the neurites. Type III beta tubulin immunoreactivity was used to identify the neurons and the accompanying mNCX-1 immunoreactive spot area confined only to neurons. Ten predetermined fields of view were sampled in each of six replicate wells per plate, with two replicate plates from different cellular preparations used for each assay. This extensive sampling of the low density cultures was conducted as some fields contained 1–3 neurons while other fields contained complex networks of 10 or more neurons. For measuring parameters of type III beta tubulin immunoreactivity and spot analysis for mNCX-1, the Cellomics Neuronal Profiling Bioapplication was used that combined spot analysis on neurons that resided within this bioapplication. For analysis of spot immunoreactivity with this bioapplication, a key parameter was the empirical establishment of fluorescent thresholding that permitted the use of a dynamic range that optimized the measurement of fluorescent differences among the treatment groups as well as distinguishing the fluorescent signal from background. This thresholding range was set

based on our previous experience with antibody-based assays and the size of the spots (1–3 μ). With this algorithm, the immunoreactive area was a relative measure that was characterized by an effective computerized spot analysis in a rapid screening mode. Importantly, the same imaging parameters for neurons from all treatment groups were employed for these studies. The key comparisons in these studies were aimed at measuring the decreases in immunoreactive area that was associated with mNCX-1, a parameter that represented the amount of knockdown for this target. Because of the observed differences in the cellular distribution of mitochondria, the cellular location of all mNCX-1 in DRG was determined, thus distinguishing the relative changes between cell bodies and neurites for this organelle. This capability and experimental focus were novel aspects of measuring the target depletion by image analysis.

Protection assay from Paclitaxel toxicity

At the conclusion of the knockdown period associated with siRNA treatment on day 9, the cultures were assessed for acute (5 hours) protective efficacy of 10 μM CBD or 100 nM KLS-13019 in preventing toxicity associated with 3 μM paclitaxel. The effective protective concentrations for the two cannabinoids were determined for other oxidative stress-related substances in previous studies (Brenneman et al., 2017). CBD and KLS-13019 were dissolved to 10 mM stock solutions in dimethyl sulfoxide and then serially diluted with sterile Dulbecco's phosphate buffered saline (DPBS; Sigma: D-5780) prior to testing. The toxic level of paclitaxel (3 μM) used for all the present studies was based on both clinically relevant serum concentrations and a previously determined toxic concentration (3 μM) that also produced increased levels of reactive oxygen species as detected with 6-chloromethyl-2',7'-dichlorodihydrofluorescein diacetate. At the conclusion of the protective assay period, sister cultures to those assessed by image analysis were evaluated with either a fluorescent dye-based assays for neuronal viability (6-carboxyfluorescein diacetate, CFDA) or with viability dye Alamar Blue. These two standard assays were chosen because CFDA has a specificity to measure neuronal viability and the Alamar Blue assay possessed increased sensitivity in comparison to CFDA. In addition, a portion of the reductive conversion of resazurin to the highly fluorescent resorufin in the Alamar Blue reagent is attributable to the action of mitochondrial reductases (Rampersad, 2012). Because of the need for enhanced sensitivity, the Alamar Blue assay was predominantly used for these studies. Similar results in assessing pharmacological responses were obtained with both assays. On every plate, wells without cells were used to provide a blank reading that was used to subtract background fluorescence. For the CFDA neuronal viability assay (Petroski and Geller, 1994), 1 mg of 6-carboxyfluorescein diacetate (CFDA) dye was dissolved in 100 mL of warm (37°C) DPBS (Gibco:D-5780) and kept in the dark until added to the brain cultures. After a complete change of medium, 100 μL CFDA dye solution was added for 15 min of incubation at 37°C in the dark. At the conclusion of the incubation period, the dye was removed from the cultures and washed once with 100 μL of DPBS. After removal of the first wash, a second wash of DPBS was added to the culture and then incubated for 30 min to allow the efflux of dye out of glia in the cultures. Selective retention of CFDA dye in neurons provided neuronal specificity to the CFDA assay. At the conclusion of the 30 min efflux period, the culture efflux medium was removed and 100 mL of 0.1% triton-X100 in

water was added to the cultures before reading at Ex490/Em517 in a CytoFluor fluorimeter. Results were expressed in relative fluorescent units (RFU). For the Alamar Blue viability assay, 10 ul of the dye was added directly to the culture well that contained 100 ul of nutrient medium (Ivanov et al., 2016). Incubation times with the dye ranged from 1–5 hrs, depending on the experimental goals. Fluorescence was measured at an excitation of 530nm and an emission of 590 on a Cytofluor plate reader. The test agents were added to the DRG cultures for a 5 hour test period. Immediately after treatment with test compound, 3 μM paclitaxel was added for the 5 hour test period.

Statistical Analysis

All statistical comparisons were made by ANOVA, with normality of values tested by the Shapiro-Wilk test followed by a multiple comparison of means test with the Holm-Sidak method as performed through Sigma plot 11. All EC_{50} and IC_{50}values were generated by the curve-fitting procedure provided by the 4 parameter Logistic analysis within Sigma plot 11.

Results

Pharmacological block of mNCX-1

CBD pharmacology is recognized to be complex with a large (>12) number of molecular targets that have been reported to mediate the varied actions of this component of cannabis. Even if the CBD targets are limited to those that have been associated with protective properties, there are still six known mediators of this action (See Brenneman et al, 2017). In contrast, the CBD analogue, KLS-13019, has more limited actions and the only known target for this new compound is mNCX-1 (Brenneman et al., 2107). Because previous studies have demonstrated that a known blocker of mNCX-1 (CGP-37157) produced a complete inhibition of neuroprotection by both cannabinoids test compounds against ethanol-mediated toxicity in hippocampal cultures (Brenneman et al, 2017), the first goal of the present work was to extend this pharmacological approach to paclitaxel toxicity in DRG cultures after demonstrating the protective effects of the two cannabinoids. As shown in figure 2A, KLS-13019-mediated protection from 3 μM paclitaxel toxicity was shown to be completely prevented during a five hour test period in a serum-free culture medium with antioxidants removed. Concentration-dependent effects of this protection are shown for the Alamar Blue viability assay with an EC50 of 18 ± 1 nM. Similar studies with KLS-13019 conducted with the CFDA neuronal viability resulted in a similar response in protecting DRG neurons with an EC50: 27 ± 6 nM (data not shown). Further, the protective effect of CBD is shown in Figure 2B, with an observed EC50 of 2.7 ± 0.4 μM. These comparative experiments indicated that while both compounds were completely efficacious in the prevention of paclitaxel-induced toxicity in DRG cultures, there was a 150-fold difference in potency between the two cannabinoids. Important to the investigation of a protective mechanism of KLS-13019 was the effect of CGP-37157 on the DRG cultures co-treated with 3 μM paclitaxel. As shown in figure 3A, an IC50 of 0.29 ± 0.11 μM was observed in preventing protection produced by 100 nM KLS-13019. Similar studies conducted with 10 μM CBD produced a similar IC50 (0.14 + 0.07 μM) in preventing protection against 3 μM paclitaxel (Figure 3B). Thus, the CGP-37157 studies indicated the concentrations producing

half-maximal decrease in protection were very similar between 10 μM CBD and 100 nM KLS-13019.

Immunofluorescent Markers in DRG Cultures

Although the protection-blocking effects of CGP-37157 were supportive of the conclusion for a mNCX-1-mediated mechanism for the two cannabinoids, additional evidence was sought using a siRNA knockdown approach to further sustain the target conclusion of mNCX-1 in protecting DRG cultures from paclitaxel. For these studies, a high content fluorescent analysis of the DRG cultures was used to investigate the use of siRNA in these complex cultures. Three immunofluorescent assays were used to assess DRG responses: 1) antiserum to type 3 beta tubulin to labeled neurons; 2) mNCX-1 immunoreactive spot analysis to measure target depletion in all DRG cells; and 3) COX4 immunoreactive spot analysis to measure changes in a marker for mitochondria. In figure 4, isolated cells and those in a network of DRG neurons are shown with these three fluorescent markers. In figure 4A, an image is shown of this cellular network with a merged fluorescence image of all the markers. In figures 4B and 4C, a similar pattern of labeling was observed with neurites and cells bodies. In Figure 4D, the COX4 assay showed labeling of all cells, but sparse and non-continuous labeling of the neurites.

Ring spot mNCX-1 analysis

A ring spot imaging paradigm was first applied to the DRG cultures. With this analysis, only the cytoplasmic region was measured for mNCX-1 IR spot area, but all cells were included. An assay of COX4 IR area was measured in this context for the ring-spot analysis (see methods section for description) in addition to the mNCX-1 IR area. An image of this spot analysis is given in Figure 5A. The respective spots for COX4 and mNCX-1 IR were detectible, albeit at low resolution. An interesting feature of the image for mNCX-1 IR was a band of IR from the nucleus to the outer limits of cytoplasmic boundary was observed in some, but not all cells. This mNCX-1 band was only observed in neurons, not non-neuronal cells as determined with co-localization with type III beta tubulin. The COX-4 IR spots were abundant in all cells. The quantitative comparison from mNCX-1 and COX4 spots areas are provided in Figure 5B. The ring-spot analysis of the cytoplasmic domain indicated a siRNA-mediated decrease in mNCX-1 IR area that was 45% of control for all cells. In contrast, there were no significant differences in COX4 immunoreactivity after treatment with mNCX-1 siRNA in comparison to controls nor was there any difference between cultures treated with non-targeted siRNA and targeted siRNA. These data indicate that the mitochondrial marker COX-4 provided a significant morphological frame of reference to study the specificity of the mNCX-1 response to siRNA. These data further support the conclusion that under these experimental conditions, neither overt toxicity nor changes in COX4 immunoreactive area were apparent after treatment with mNCX-1 siRNA in these morphological assays of mitochondria.

Neuronal Target Knockdown of mNCX-1

An image of an isolated DRG neuron is shown stained by immunofluorescence with type3 beta tubulin 4 days after mNCX-1 siRNA treatment in figure 6A. The same neuron stained for both type 3 beta tubulin and mNCX-1is shown in figure 6B. In this image, the sensory

neuron was depicted with a prominent cell body and two neurites. In contrast, an image of several control neurons is shown for neuronal labeling in figure 6C and in combined neuronal and mNCX-1 labeling in figure 6D. While these images are suggestive of a loss of mNCX-1 immunoreactive area in the neurites of siRNA-treated cultures in comparison to the controls, quantitative image analysis measures of mCNX-1 immunoreactive spot areas are shown for both neurons and cell bodies in figure 7A. In this representative data from one experiment, a 53 ± 3 % decrease in cell body immunoreactive spot area for mNCX-1 was observed in siRNA-treated cultures in comparison to controls. This finding was typical for all the siRNA experiments in which a 52–55 % decrease in cell body mNCX -1 area was observed. An unanticipated finding was observed for the neurites of siRNA-treated cultures. Although the amount of mNCX-1 IR area in neurites was only 14% of that observed in the cell bodies in the siRNA-treated cultures, a significantly ($P < 0.001$) greater loss of (72 ± 2%) IR area in the neurites was observed in comparison to neurites from control neurons. This finding was typical for all the siRNA experiments in which a 67–82 % decrease in neurite mNCX -1 area was observed in comparison to control neurites. Again, this preferential loss of IR area in the neurites in comparison to that occurring in the cell bodies was a consistent finding in all of the mNCX-1-targeted siRNA experiments. A non-targeted siRNA was also tested as a control for specificity. As shown in figure 7B, the non-targeted control siRNA produced no detectible change in the mNCX-1 immunoreactive area in comparison to that of control cultures. As observed in the targeted siRNA studies, most (80%) of the immunoreactivity of mNCX-1 in controls resided in the cell bodies.

siRNA knockdown and protective activity

In the previous section, the results indicated a preferential decrease in neurite IR area observed in cultures treated with siRNA to mNCX-1 over that course of 5 days of siRNA treatment and target silencing (70–80%); whereas the cell bodies exhibited a more modest 50–55% decrease in mNCX-1 IRA area. The fundamental question remained to be addressed: what was the effect of siRNA treatment on cannabinoid-mediated protection from paclitaxel toxicity? In figure 8A, a representative experiment is shown that indicates that a significant decrease (82 ± 2 %) in the protective signal was observed after treatment with 1 μM siRNA. To be clear on the neuroprotective assay, this experiment was performed on day that was 4 days after treatment with the siRNA. Importantly, the culture medium was changed into a B27/neurobasal medium that was formulated without antioxidants. This paradigm was chosen to both decrease the nutrient medium-related background for antioxidants and to permit a rapid and reproducible test system to both measure a robust toxic response of 3 μM paclitaxel as well as provide a means to perform a measure of protective efficacy for the two test cannabinoids. As shown in figure 8A, paclitaxel treatment alone produced a toxic signal of 4065 fluorescent units (a 32% decrease from that of the positive control (KLS-13019 + paclitaxel). This toxic signal was typical for these experiments that ranged from 29–34% of control. As shown, treatment with 100 nM KLS-13019 plus paclitaxel produced Alamar Blue fluorescence that was not statistically different from that of control cultures. Importantly, the addition of mNCX-1 siRNA to the cultures that were co-treated with 3 μM paclitaxel and 100 nM KLS-13019 exhibited a diminished fluorescence that was significantly less (3348 fluorescent units) from that of the cultures with 100 KLS-13019 and 3 μM paclitaxel. This 82% decrease in fluorescence from

the protective signal was similar to those of other experiments with 100 nM KLS-13019 or 10 μM CBD as shown in Figure 8B. In this summary, the comparison of all experiments demonstrated that the percentage decreases observed from the respective positive controls (paclitaxel + cannabinoid) as compared with percentage decreases in neurite mNCX-1 IR area were very similar. These data strongly indicate a similarity between decreased responses in protection from paclitaxel mediated by cannabinoids and the respective decreased amount of neuritic mNCX-1 IR target area across all experiments.

Non-toxic mNCX-1 siRNA

Fundamental to the interpretation of the siRNA results was the demonstration that this treatment did not produce toxicity under the experimental conditions described. In figure 9, a summary of data on viability dye responses and high content-derived parameters are presented indicating no toxic effects were detected on day 9, the conclusion of the 4 day knockdown period. In arguably the most definitive measure, a time course of the Alamar Blue viability assay is presented in figure A showing a comparison between control cultures and those treated with mNCX-1 siRNA as previously described. As observed hourly over a 5 hour test period, there were no significant differences in the Alamar Blue viability assay between cultures treated with mNCX-1 siRNA and controls. In addition to the viability assay, multi-parametric arrays of neuronal assay were also conducted by high content imaging of the DRG neurons. All of the assays shown in figure 9B indicated no statistically different decrease in comparison to the corresponding measured in control cultures. In addition to the data obtained on the day 9 cultures, similar studies were also conducted immediately after siRNA retreatment on day 5. The results conducted at this earlier stage of treatment also indicated no toxicity as measured by the Alamar Blue viability in comparing control cultures to those treated for 24 hours with mNCX-1 siRNA (data not shown). Together, the viability assays and the high content image analyses indicated that the mNCX-1 siRNA treatment did not produce statistically significant toxicity in the DRG cultures.

Discussion

CIPN and Paclitaxel

Many chemotherapeutic agents elicit significant neuropathies severe enough to ultimately result in the cessation of treatment. The incidence of CIPN has been reported to occur in 30–40% of patients (Seretny et al., 2014). While this effect is not confined to a single class of drugs, the present study as focused on paclitaxel, a taxane-derived chemotherapeutic agent used for the treatment of a variety of solid tumors. The primary anti-cancer action of paclitaxel is believed to occur by binding to the β-tubulin subunit in microtubules causing a disruption of the mitotic spindle and suppression of microtubule dynamics. The resulting action on tumors is cell cycle arrest and apoptosis of proliferating cells (Jordan et al., 1993; Xiao et al., 2006). This toxic effect on tumors is in contrast to the actions produced on neurons that account for the complications in CIPN. For example, paclitaxel toxicity has been associated with three key effects: mitochondrial dysfunction, lose of calcium homeostasis, oxidative stress (Han and Smith, 2013). All of these toxicities appear to occur on sensory neurons located in the dorsal root ganglia and all of these effects can have a

mitochondrial basis. In animal models, paclitaxel has been shown to accumulate in DRG and produce measurable amounts of reactive oxygen species (Duggett et al., 2016). These findings identify DRG cultures as a compelling experimental choice for the studies of CIPN and as an accessible model to evaluate protective mechanisms from potential therapeutics focused on preventing this side-effect. As our treatment strategy focused on the very early (3–5 hours) toxic responses to paclitaxel, the concept was to prevent the toxicity before neuronal responses became irreversible and more complex. This strategy further suggests that a prophylactic treatment schedule beginning before the administration of chemotherapeutic agents might be of long term and protective benefit.

These studies do not address cannabinoid mechanisms which may account for protection from more chronic aspects of the paclitaxel toxicity and neuropathic pain that is evident in CIPN. More chronic treatment with paclitaxel has been associated with both inhibition of axonal transport and the neurite retraction that occur 1–3 days after paclitaxel treatment (Guo et al., 2017; Gornstein and Schwarz, 2017). In the present study, there was no evidence for decreases in neurite length or decreases in neuritic complexity (See figure 9) after the 5 hour treatment with paclitaxel. In regard to potential changes in axonal transport of mitochondria, there was a small decrease (10%) in COX4 immunoreactivity in neurites that did not reach the level of statistical significance (see figure 9). If confirmed in future experiments, a small change in COX4 could be attributed to either decrease in axonal transport or toxicity. Thus, it cannot be ruled out that there was an effect on axonal transport or toxicity in a subpopulation of sensory neurons. Of potential relevance is the observation that paclitaxel treatment of pheochromocytoma cultures produced a decrease in mitochondrial mobility within 2–3 hours (Shprung and Gozes, 2009). Further studies of the acute effects of paclitaxel on axonal transport in sensory neurons are merited to resolve this possibility and it relevance to CIPN (see Gornstein and Schwarz, 2017).

Cannabinoids and CIPN

Although the use of medical cannabis and CBD has achieved an anecdotal level of acceptance by many caregivers, the treatment for neuropathic pain, like most others, has lacked a demonstration of efficacy in a clinical trial. While verifiable the human data has yet to be achieved, significant efficacy has been reported in animal models of CIPN focused on mechanical and cold allodynia in rodents treated with paclitaxel (Ward et al., 2014). These studies, which have focused on the ability of CBD to prevent the onset of allodynia associated with paclitaxel treatment, provided supportive evidence in a reproducible model that has driven our interest in this area. While the CBD-related results provided evidence of preventative efficacy, significant concerns on the drug-like properties of CBD limited this compound as a potential therapeutic. Among the pharmacological concerns for CBD were the lack of bioavailability after oral administration and the low potency (10 μM) of CBD in primary neuronal system that was vulnerable to oxidative stress (Brenneman et al., 2017). With the discovery of KLS-13019, many of the concerns were addressed by the enhanced properties of the new compound showing: a 150-fold increase in potency in preventing toxicity, a 5-fold decrease in toxicity *in vitro*, an 8-fold increase in oral bioavailability and a more focused pharmacology on preventing toxicity associated with oxidative stress. Because of the demonstrated overlap in protective efficacy and the fact that the KLS-13019 was

based on the CBD core structure, these two cannabinoids were chosen to compare their potency, efficacy and mechanism of action in DRG cultures treated with a low concentration of paclitaxel in acute toxicity assays in DRG cultures.

Mitochondrial NCX-1 and protective cannabinoids

The fundamental choice of mNCX-1 as a target for protection from paclitaxel was based on the importance of calcium homeostasis in determining neuronal damage and death. Although this target is associated with regulation of mitochondrial calcium, the complexity of this target was potentially confounding in that this exchanger can act to extrude calcium from the mitochondria or act in a reverse mode to allow more calcium into the mitochondrial matrix. This duality of function, while poorly understood, provides a target of great potential importance in neuronal injury. It is of interest that mNCX-1 is a member of a family of exchangers that have been identified as having effects on neuroprotection in a variety of cells and neuropathological diseases (Sisalli et al., 2014); Molinaro et al., 2016). The fact that the knockout of mNCX-1 has been shown to produce embryonic lethality by the cessation of cardiac function (Cho et al., 2003) confirmed the critical nature of this regulatory protein, yet providing concerns on the potential toxic consequences in blocking or attenuating the expression of mNCX-1. Because of this known liability of mNCX-1 target knockout in cardiac cells, substantial evidence was obtained to monitor viability responses of DRG cultures after siRNA knockdown. While the present studies in DRG cultures indicated that the action of cannabinoids can be substantially altered by the expression levels of NCX-1, the exact nature and level of cannabinoid interactions directly with the target remain ongoing areas of investigation. These studies do not rule an indirect action of the cannabinoids acting on a regulatory effector of mNCX-1 to account for the protective action; rather, these data indicate that mNCX-1 is, at minimum, an obligatory component of the cannabinoid mechanism.

Assessment of siRNA effects

This study has provided evidence for both the comparison of changes in protective activity associated with two cannabinoids and changes in the immunoreactivity of mNCX-1 target in a complex and relevant model of sensory neurons derived from embryonic rat dorsal root ganglion. Of prime importance was to evaluate the level of decrease in the protective efficacy after siRNA treatment. Because preliminary experiments indicated that there was a substantial and reproducible toxic effect of 3 μM paclitaxel in day 8 DRG cultures, this acute toxicity formed the basis for evaluating the protective effects of the cannabinoid in preventing this toxicity. This is an important feature of these experiments, as they focus on early toxic effects that may be distinct from more chronic studies which have resulted in loses of neuronal structures with more prolonged treatment (1–3 weeks) and higher concentrations of paclitaxel in DRG cultures (Chen et al., 2015). Our perspective was that while both acute and chronic effects need to be evaluated in CIPN, our target-related studies on siRNA effects focused only on the acute paradigm that provided a practical approach to evaluating the siRNA effects while potentially avoiding confounding and potentially more complicated toxic effects resulting from a more prolonged treatment.

High content fluorescence imaging of the DRG cultures provided necessary technical capabilities for non-biased sampling of the complexities of sensory neuron responses to the siRNA treatment. The initial studies focused on the immunoreactive area of mNCX-1 were directed to the cell bodies, the location of the majority of mitochondria. However, this initial analysis indicated that there was only a 50–55% reduction in the mNCX-1 area 4 days after treatment with the siRNA. This reduction was in contrast to a 70–82% decrease in the protective activity mediated by either CBD or KLS-13019 treatment. This large disparity between target depletion and target activity provided the impetus to examine further the responses of the DRG neurons. In another series of studies, the entire neuron was examined for changes in immunoreactive area that included the neurites. This expansion resulted in an unexpected finding: the percentage (70–80%) knockdown of target in the neurites far exceeded that observed for the cell bodies. Thus, a very close agreement was observed between the loss of mNCX-1 target area in the neurites was observed that corresponded closely to the loss of acute protective activity in day 9. However, this close correspondence between target knockdown in neuritic mitochondria and the observed decrease in protection does not negate the possibility of other targets contributing to the protection provided by these cannabinoids or suggest that mitochondria within the cell bodies do not contribute to the protective mechanism. Rather, the present studies suggest that the NCX-1 in neuritic mitochondria is a plausible and sufficient mechanism for the cannabinoid protection of sensory neurons from paclitaxel.

Because toxicity was a potential outcome that would negate the interpretation of the target-mediated activity, the effect of siRNA treatment on neuronal and cellular viability was conducted 24 hours after siRNA (day 5) and on day 9, right before the 5 hour test of cannabinoid-mediated protection from paclitaxel. On both days of testing, there was no evidence by either assay for siRNA-mediated toxicity. Based on these findings, it was concluded that toxicity did not play a significant role in confounding the interpretation of the studies: mNCX-1 target knockdown in the neurites correlated well with the loss of protective activity associated with cannabinoid-mediated protection from paclitaxel.

Mitochondrial heterogeneity and cannabinoid responses

The high content analysis of DRG responses to siRNA indicated a regional difference in immunoreactive response, with the neurites being far more responsive than the cell body mitochondria. Evidence for the heterogeneity of mitochondria between cell bodies and neurites has been reported for DRG neurons (Kuznetsov and Margreiter, 2009). Previous studies (Dedov and Roufogalis, 1999) indicated that the neurite mitochondria were smaller and far more mobile, exhibiting a greater mitochondrial membrane potential (Delta Psi). Indeed, others have noted that “synaptic mitochondria” located in the neurites were likely involved in the providing support required for neurotransmission and synaptic plasticity (Fedorovich et al., 2017; Kulbe et al., 2017). Emerging from this concept was a hypothesis that these “synaptic mitochondria” may be ultimately the locus for cannabinoid-mediated protection and calcium regulation. This concept of specialized mitochondria being the site of drug action may provide a clue about the complex pharmacology for these cannabinoids.

Summary—Based on the high content analysis of decreases in mNCX-1 immunoreactive area in DRG neurons, the siRNA approach confirmed the importance of this target in producing acute (5 hour) protective actions of CBD and KLS-13019. Coupled with the pharmacological studies, the target knockdown observations suggested that with both cannabinoids, the mNCX-1 target was sufficient to mediate the protection from toxicity produced by paclitaxel in sensory neurons. An unexpected finding was the identification of neuritic mitochondria as a target for the protective action of these cannabinoids. A working hypothesis emerging from these studies is that the cellular location of a target may be of equal importance to the identity of that target, thereby completing or helping to define the mechanistic concept.

Acknowledgment:

These studies were supported by a Grant from the National Institute On Drug Abuse of the National Institutes of Health (R41DA044898).

References

Argyriou AA, Kyritsis AP, Makatsoris T and Kalofonos HP (2014) Chemotherapy-induced peripheral neuropathy in adults: a comprehensive update of the literature. Cancer Manag. Res 6:135–147. [PubMed: 24672257]

Bih CI, Chen T, Nunn AVW, Bazelot M, Dallas M, Whalley BJ (2015) Molecular targets of cannabidiol in neurological disorders. Neurotherap 12: 699–730.

Blaustein MP, Lederer WJ (1999) Sodium/calcium exchange: its physiological implications. Physiol Rev 79:763–854. [PubMed: 10390518]

Brenneman DE, Smith GR, Zhang Y, Du Y, Kondaveeti SK, Zdilla MJ, Reitz AB (2012) Small-molecule anticonvulsant agents with potent in vitro neuroprotection. J Mol Neurosci 47:368–379. [PubMed: 22535312]

Brenneman DE, Petkanas D, Kinney WA (2017). Pharmacological comparisons between cannabidiol and KLS-13019. J Mol Neurosci 66:121–124.

Brewer GJ, Torricelli JR, Evege EK, Price PJ (1993) Optimized survival of hippocampal neurons in B27 supplemented Neurobasal, a new serum-free medium combination. J. Neurosci. Res 35:567–576. [PubMed: 8377226]

Canta A, Pozzi E, Carozzi VA (2015). Mitochondrial dysfunction in chemotherapy-induced peripheral neuropathy (CIPN). Toxics 3: 198–223, [PubMed: 29056658]

Celsi F, Pizzo P, Brini M, Leo S, Fotino C, Pinton P, Rissuto (2009) Mitochondria, calcium and cell death: a deadly triad in neurodegeneration. Bioch. Biophys Acta 1787:335–344.

Chen L-H, Sun Y-T, Chen Y-F, Lee M-Y, Chang L-Y, Chang J-Y, Shen M-R (2015). Integrating image-based high-content screening with mouse models identifies 5-hydroxydecanoate as a neuroprotective drug for paclitaxel-induced neuropathy. Mol Cancer Therp 14:2206–2214.

Cho CH, Lee SY, Shin HS, Philipson KD, Lee CO (2003). Partial rescue of the Na+Ca2+ exchanger (NCX1) knock-out mouse by transgenic expression of NCX1. Exp Mol Med 35:125- [PubMed: 12754417]

Darkovska-Serafimovska M, Serafimovska T, Arsova-Sarafinovska Z, Stefanoski S, Keskovski Z, Balkanov T. (2018) Pharmacotherapeutic considerations for use of cannabinoids to relieve pain in patients with malignant diseases. J Pain Res 11: 837–842. [PubMed: 29719417]

Dedov VN, Roufogalis BD (1999). Organization of mitochondria in living sensory neurons. FEBS Letters 456:171–174. [PubMed: 10452552]

Duggett NA, Griffiths LA, McKenna OE, De Santis V, Yongsanguanchai N, Mokori EB Flatters SJL (2016) Oxidative stress in the development, maintenance and resolution of paclitaxel-induced painful neuropathy. Neurosci 333:13–26.

Fedorovich SV, Waseem TV, Puchkova LY (2017) Biogenetic and morphofunctional heterogeneity of mitochondria: the case of synaptic mitochondria. Rev. Neurosci 28:363–373. [PubMed: 28195557]

Gornstein EL and Schwarz TL (2017) Neurotoxic mechanisms of paclitaxel are local to the distal axon and independent of transport defects. Exp Neurol 288: 153–166. [PubMed: 27894788]

Guo L, Hamren J III, Eldridge S, Behrsing HP, Cutuli FM, Mussio J, Davis M (2017). Multiparametric image analysis of rat dorsal root ganglion cultures to evaluate peripheral neuropathy-inducing chemotherapeutics. Tox Sci 156:275–288.

Han Y, Smith MT (2013) Pathobiology of cancer chemotherapy-induced peripheral neuropathy (CIPN) Front. Pharmacol. 4: (156) 1–16.

Ivanov DP, Al-Rubai A, Grabowska AM, Pratten MK (2016). Separating chemotherapy-related developmental toxicology from cytotoxicity in monolayer and neurosphere cultures of human fetal brain cells. Tox in Vitro 37:88–96.

Jordan MA, Toso RJ, Thrower D, Wilson L (1993). Mechanism of mitotic block and inhibition of cell proliferation by Taxol at low concentrations. PNAS (USA) 90:9552–9556. (see Duggett) [PubMed: 8105478]

King KM, Myers AM, Soroka-Monzo AJ, Tuma RF, Tallarida RJ, Walker EA, Ward SJ (2017). Single and combined effects of Δ^9-tetrahydrocannabinol and cannabidiol in a mouse model of chemotherapy-induced neuropathic pain. Brit J Pharmacol 174:2832–2841. [PubMed: 28548225]

Kinney WA, McDonnell ME, Zhong HM, Liu C, Yang L, Ling W, Qian T, Chen Y, Cai Z, Petkanas D, Brenneman DE (2016) Discovery of KLS-13019, a Cannabidiol-Derived Neuroprotective Agent, with Improved Potency, Safety, and Permeability" ACS Med. Chem. Lett 7: 424–428.

Kulbe JR, Hill RL, Singh IN, Wang JA, Hall ED (2017) Synaptic mitochondria sustain more damage than non-synaptic mitochondria after traumatic brain injury and are protected by cyclosporin A. J Neurotrauma 34:1291–1301. [PubMed: 27596283]

Kuznetsov AV, Margreiter R (2009) Heterogeneity of mitochondria and mitochondrial function within cells as another level of mitochondrial complexity. Int J Mol Sci 10:1911–1929. [PubMed: 19468346]

Lim K, See YM, Lee J. (2017). A systematic review of the effectiveness of medical cannabis for psychiatric, movement and neurodegenerative disorders. Clin Psychopharm Neurosci 15:301–312,

Molinaro P, Sirabella R, Pignataro G, Petrozziello T, Secondo A et al. (2016). Neuronal NCX1 overexpression induces stroke resistance while knockout induced vulnerability via Akt. J Cerebral Blood Flow 36:1790–1803.

Palty R, Silverman WF, Hershfinkel M, Caporale T, Sensi S, Parnis J, Nolte C, Fishman D, Shoshan-Barmatz V, Herrmann S, Khananshvili D, Sekler I. (2010) NCLX is an essential component of mitochondrial Na+Ca2+ exchange. PNAS (USA) 107:436–441. [PubMed: 20018762]

Petroski RE, Geller HM (1994) Selective labeling of embryonic neurons cultures on astrocyte monolayers with 5(6)-carboxyfluorescein diacetate (CFDA). J. Neurosci. Methods 52:23–32. [PubMed: 8090014]

Rampersad SN (2012). Multiple applications of Alamar Blue as an indicator of metabolic function and cellular health in cell viability bioassays. Sensors 12:12377–12360.

Ryan D, Drysdale AJ, Lafourcade C, Pertwee RG, Platt B (2009). Cannabidiol targets mitochondria to regulate intracellular Ca2+ levels. J Neurosci 29: 2053–2063. [PubMed: 19228959]

Seretny M, Currie GL, Sena ES, Ramnarine S, Grant R, MacLeod MR, Colvin LA, Fallon M. (2014). Incidence, prevalence, and predictors of chemotherapy-induced peripheral neuropathy: a systematic review and meta-analysis. Pain 155:2461–2470. [PubMed: 25261162]

Shprung T and Gozes I (2009) A novel method for analyzing mitochondrial movement: inhition by paclitaxel in a pheochromocytoma cell model. J Mol Neurosci 37:254–262. [PubMed: 18636346]

Sisalli MJ, Secondo A, Esposito A, Valsecchi V, Savola C, Di Renzo GF et al. (2014) Endoplasmic reticulum refilling and mitochondrial calcium extrusion promoted in neurons by NCX1 and NCX3 in ischemic preconditioning are determinant for neuroprotection. Cell Death and Differentiation 21:1142–1149 [PubMed: 24632945]

Ward SJ, Ramirez MD, Neelakantan H, Walker EA (2011) Cannabidiol prevents the development of cold and mechanical allodynia in paclitaxel-treated female C57Bl6 mice. Anesh Analg 113: 947–950.

Ward SJ, McAllister SD, Kawamura R, Murase R, Neelakantan H, Walker EA (2014) Cannabidiol inhibits paclitaxel-induced neuropathic pain through 5-HT1A receptors without diminishing nervous system function or chemotherapy efficacy. Brit J Pharmacol 171: 636–645. [PubMed: 24117398]

Ward SJ, Riggs D, Tuma R, Kinney WA, Petkanas D. Brenneman DE (2017). Neuroprotective and anti-inflammatory effects of KLS-13019 and cannabidiol in in vitro and in vivo models of chemotherapy-induced neuropathic pain. International Cannabinoid Research Society Symposium, 6 22, 2017, Montreal, Canada, 27: P1–40.

Xiao H, Veridier-Pinard P, Fernandez-Fuentes N, Burd B, Angeletti R et al. (2006) Insights into the mechanism of microtubule stabilization by Taxol. PNAS (USA) 103:10166–10173. [PubMed: 16801540]

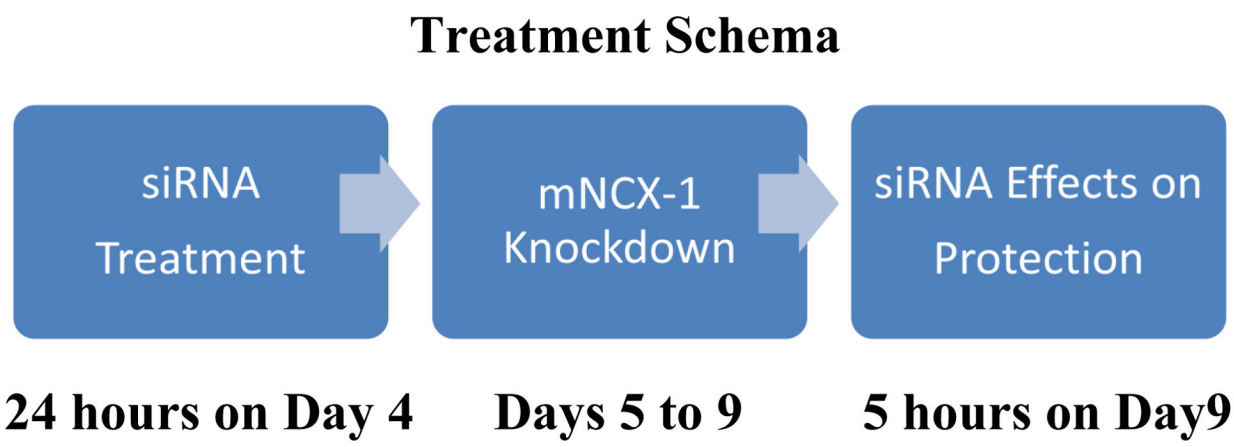

Fig. 1.

Treatment schema for dorsal root ganglion cultures and mNCX-1 siRNA. Three periods of siRNA treatment and their respective treatment durations are shown. Each treatment period is terminated with a complete change of a culture medium corresponding with the stage of siRNA treatment. At the conclusion of the 5 hour assay on protection from paclitaxel on day 9, the cultures were assessed for loss of protection from paclitaxel toxicity produced by the two cannabinoids and for the depletion of the mNCX-1 target.

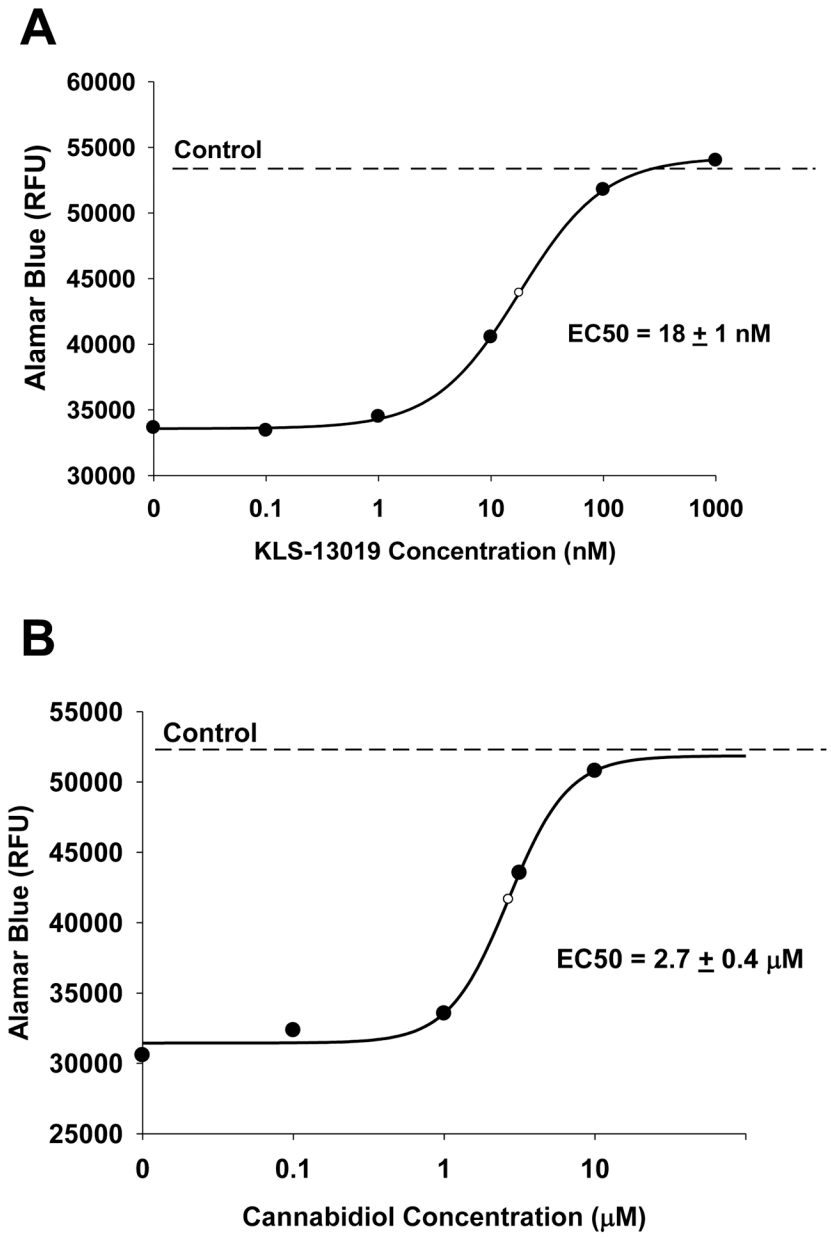

Fig. 2.

Determinations of efficacy and potency (EC50 ± standard error) are shown for protection against paclitaxel-induced toxicity after treatment with KLS-13019 (part A) or cannabidiol (part B). The EC50 was determined from a curve fitting procedure by a 4-parameter logistic analysis. Each value is the mean of 5 determinations at each concentration. The standard errors for the data points ranged from 4–6% of the mean. A representative experiment from two replicate experiments is shown. Dorsal root ganglion cultures were tested during a five hour treatment period on day 9 in culture. All cultures received a complete change of medium before treatment was initiated. The dashed line is a reference line of the Alamar Blue response from control cultures The Alamar blue value at zero concentration of test agent represents the culture response to 3 μM paclitaxel treatment alone.

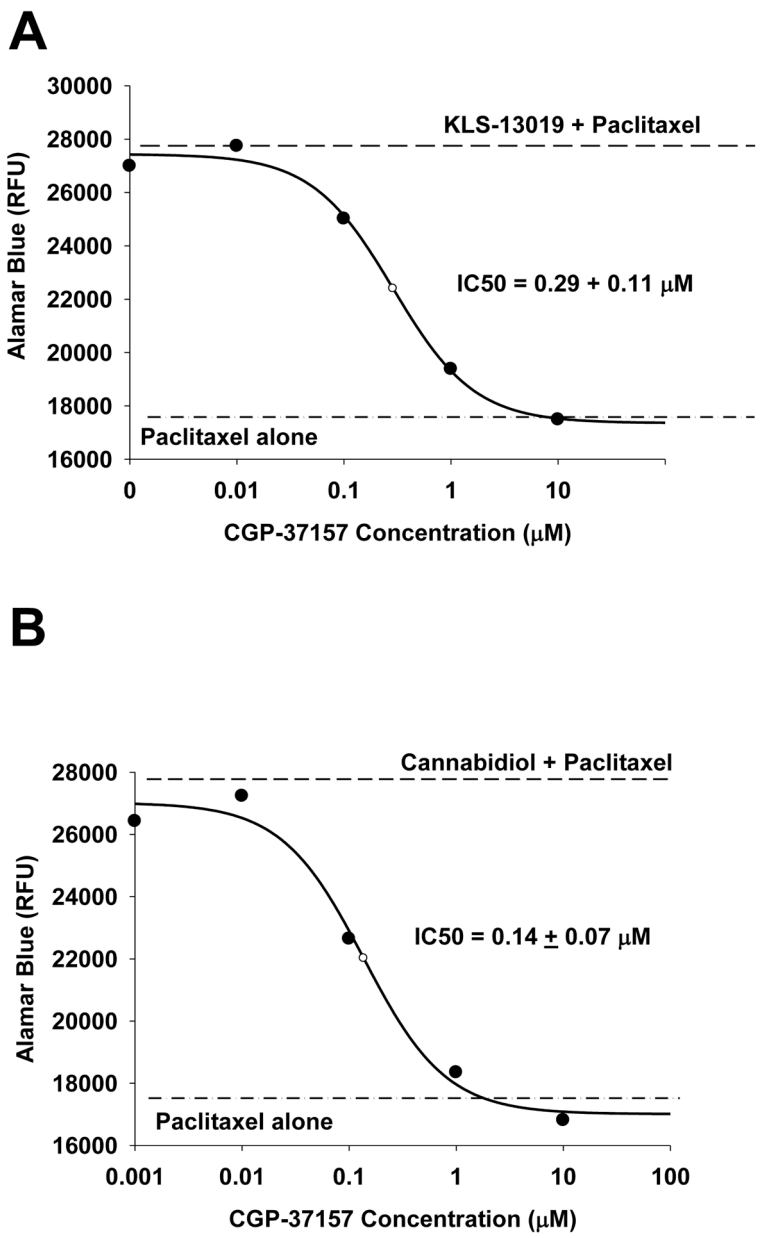

Fig. 3.

The IC50 for CGP-37157 (a mNCX-1 inhibitor) is compared for 100 nM KLS-13019 (part A) and 10 μM cannabidiol (part B) in dorsal root ganglion cultures treated for 5 hours on day 9 in culture. The IC50 ± the standard error were determined from a curve fitting procedure by a 4-parameter logistic analysis. Each value is the mean of 5 determinations at each concentration. The standard errors for the data points ranged from 4–7% of the mean. A representative experiment from two replicate experiments is shown. The dashed line represents the Alamar Blue fluorescence value for cultures treated with the respective test agent and 3 μM paclitaxel, with the control value being at zero CGP-37157 concentration. The dash-dot-dash line is the fluorescence response of cultures treated only with 3 μM paclitaxel.

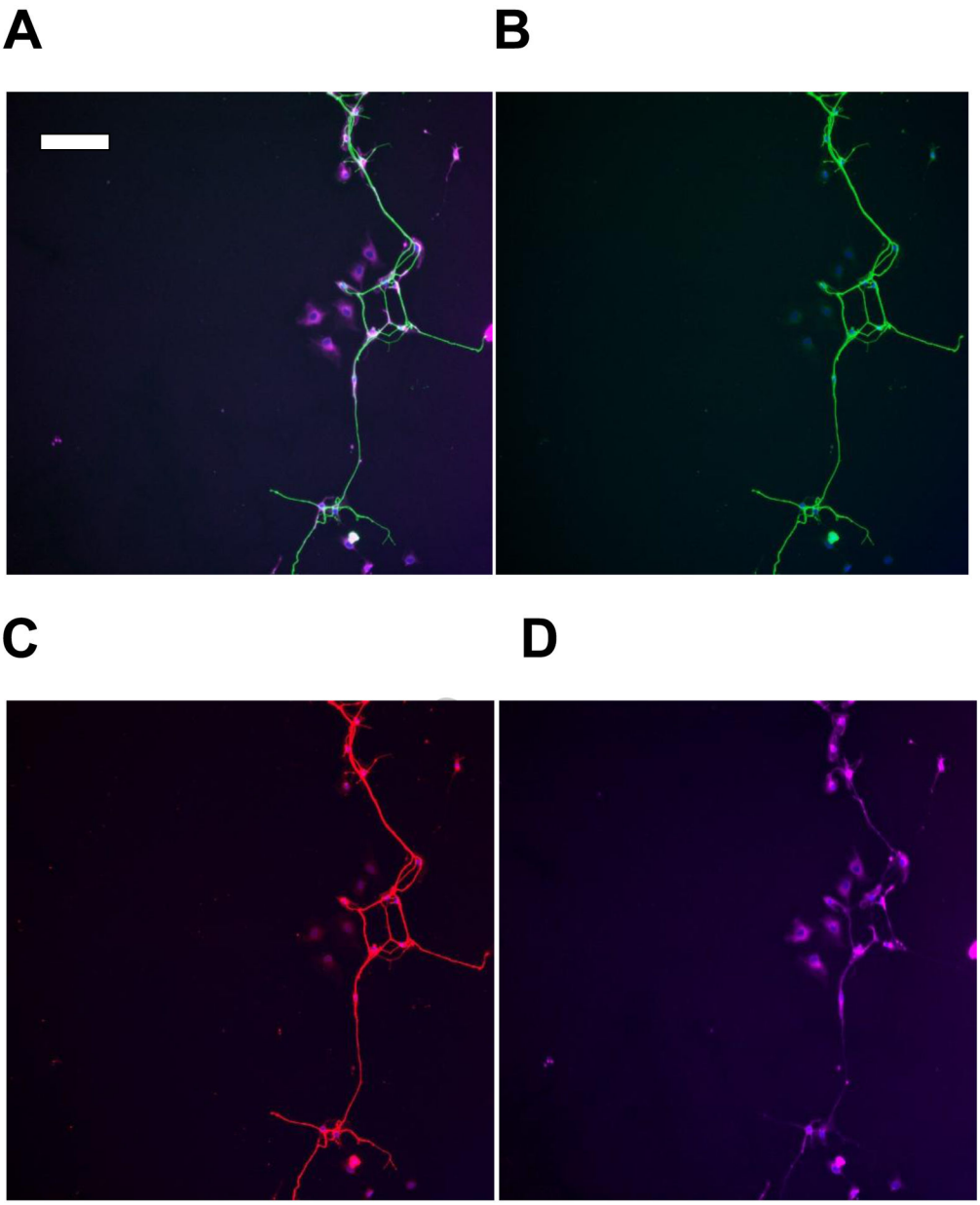

Fig. 4.

Immunofluorescent labeling images of a dorsal root ganglion network of control cells are shown for a day 9 culture. In part A, the composite of all fluorescent labeling is shown that included type III beta tubulin for neurons (part B), mNCX-1 (part C) and COX4 for mitochondria (part D). These images were taken with similar fluorescence thresholding values. The calibration bar shown in panel A represents 100 μ.

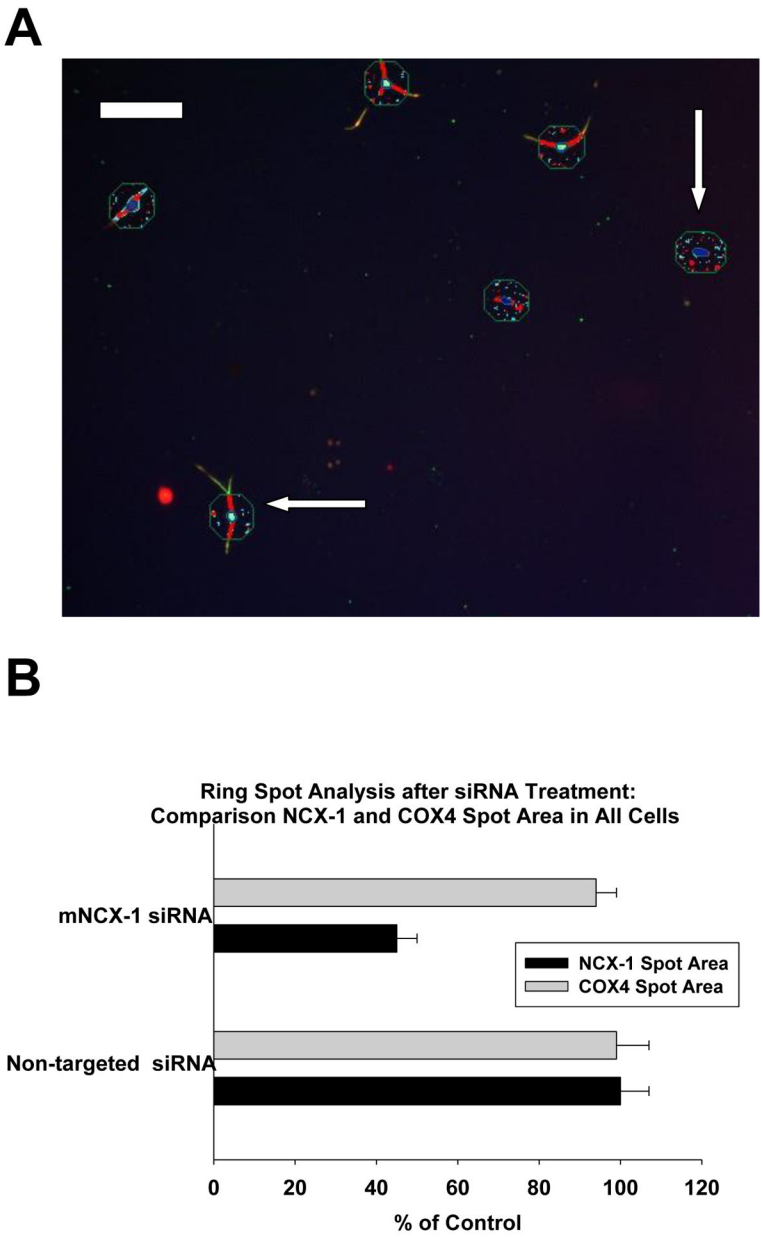

Fig. 5.

Ring spot image analysis of dorsal root ganglion cultures on day 9 after plating (part A). The punctate spot imaging is of the cytoplasmic domain and the nucleus of all cells. Mitochondria-related spots (blue) were identified with COX-4 immunofluorescence and mNCX-1 –related spots are shown in red. Both neuronal cells (horizontal arrow) and non-neuronal cells (vertical arrow) are shown for comparison. This ring spot region was initially chosen because of the predominant location of mitochondria in the cell bodies of neurons, and the non-neuronal cells were displayed for comparative purposes. The calibration bar shown in panel A represents 100 μ. In panel B, a comparison of mNCX-1 spot area (black bars) and COX-4 spot area (gray bars) are shown for all cells in cultures treated with siRNA to mNCX-1 or to non-targeted siRNA. All data are expressed as a percentage of values from

control cultures. The siRNA treatment paradigm was conducted as described in figure 1. The error bars are standard errors and the bars represent the mean of 5 determinations from a representative experiment from two replicate studies.

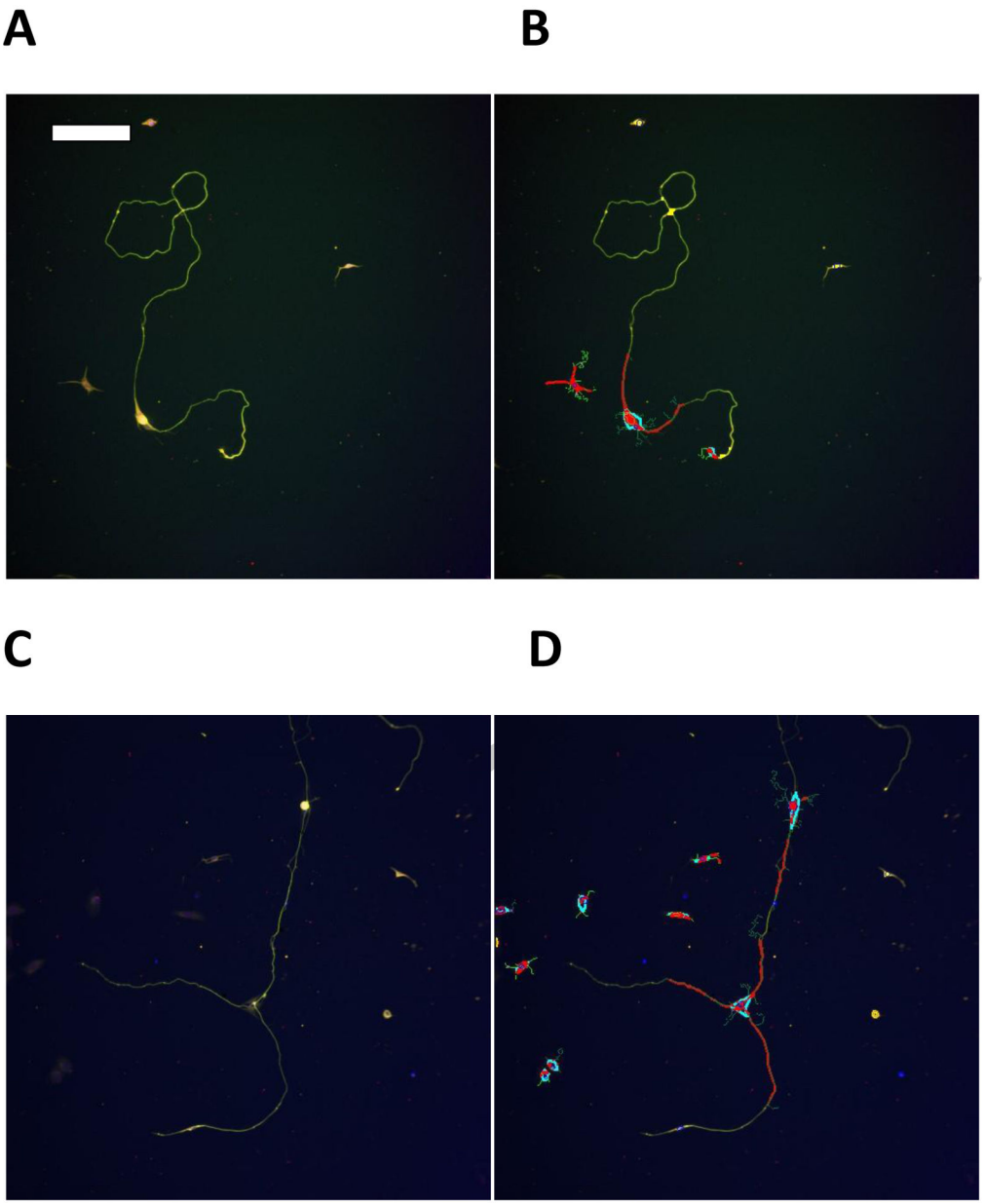

Fig. 6.

In part 6A, a DRG neuron is shown after treatment with mNCX-1 siRNA for 4 days after removal of the siRNA (see Figure 1). DRG cultures have been treated with antibodies to type 3 beta tubulin and stained with a secondary body labeled with Alexa dye 488 to display the neuronal structure (green). In part 6B, the same neuron has been co-stained with antibodies to mNCX-1 and a secondary antibody labeled with Alexa dye 555 (red). For a comparative purposes, the same reagents as utilized in siRNA -treated cultures (6A and 6B), control neurons of the same maturity were stained with type 3 beta tubulin in 6 C and in combination with mNCX-1 and type 3 beta tubulin immunofluorescence (green) in 6 D. The calibration bar represents 100 μ.

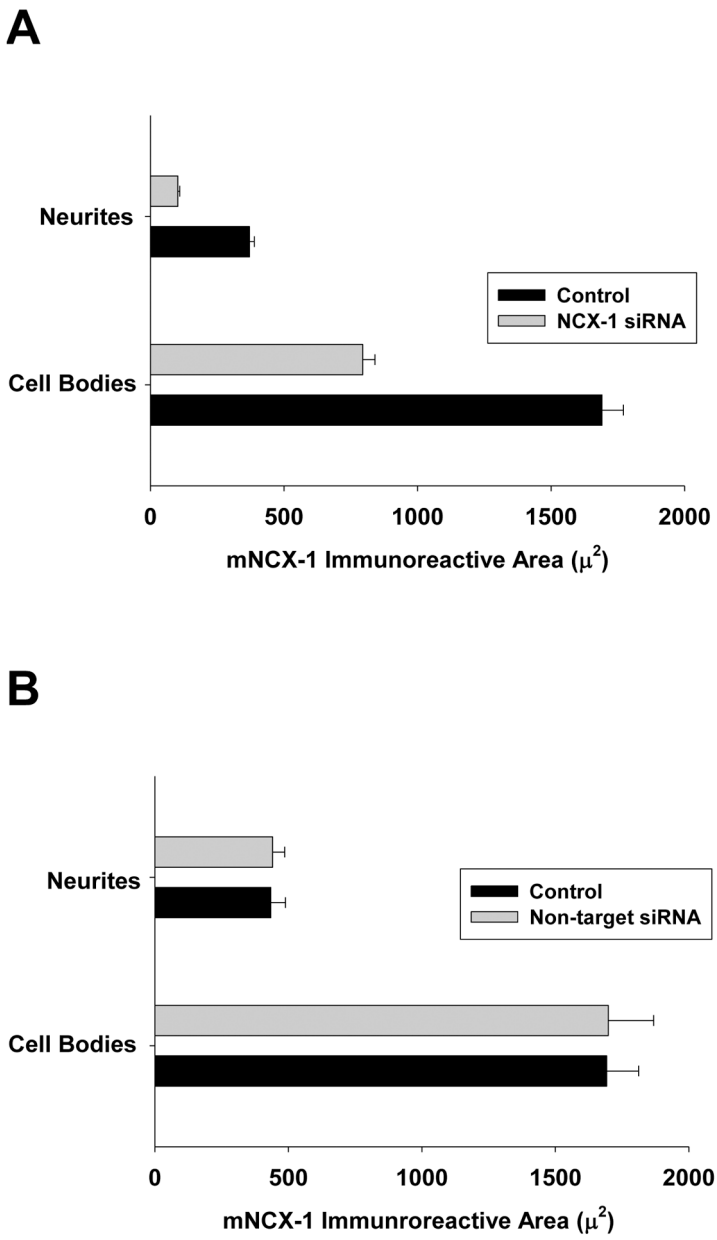

Fig. 7.

In part A, the immunoreactive area of mNCX-1 was compared between cultures treated with siRNA to mNCX-1 and controls after a 4 day knockdown period following siRNA treatment. In these data from a representative experiment, the immunoreactive spot area for mNCX-1 is compared between that occurring in cell bodies (two lower bars) and that occurring in neurites (upper two bars) as determined from the neuronal profiling image analysis bioapplication. Each bar is the mean of values from 10 fields from each of six replicate culture wells (60 fields total) and the error bar is the standard error of the mean. For both neurons and cell bodies, siRNA treatment produced a significant decrease in mNCX-1 immunoreactive spot area from that of their respective control values, although the % decrease in neurites (72 ± 2) was far greater than that observed for cell bodies (55 ± 3). In

part B, similar comparisons were made as that described in part A, except non-targeting siRNA was tested. In contrast to that observed with mNCX-1 siRNA, there were no statistically different effects of the non-targeting siRNA on either cell bodies or neurites in comparison to their respective controls. Each bar is the mean of values from 10 fields from each of 6 replicate wells and the error bar is the standard error of the mean. The presented data is a representative experiment from duplicate studies.

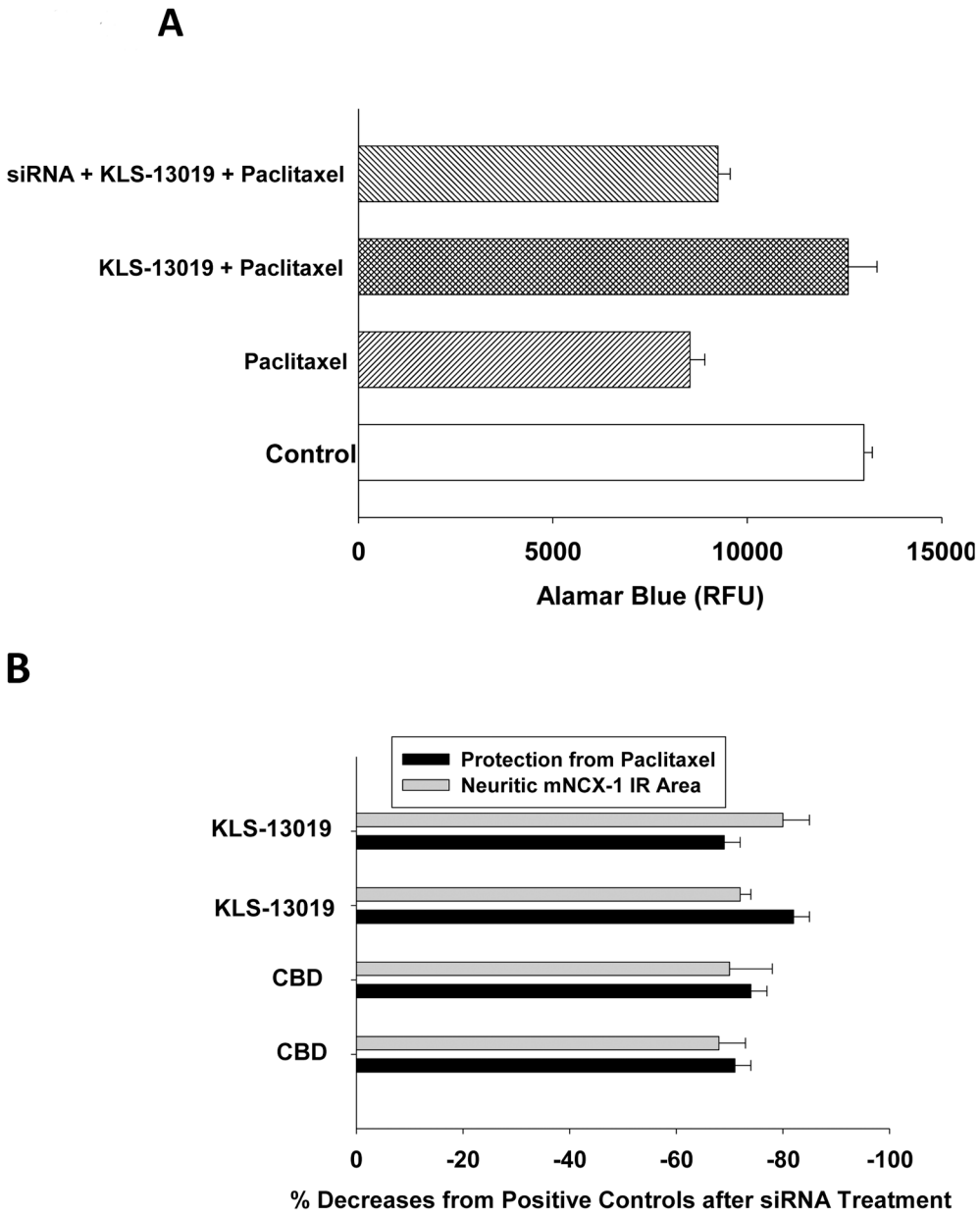

Fig 8.

Part A Effect of KLS-13019 on paclitaxel-induced decreases in fluorescence from the viability dye Alamar Blue during a 5 hour test period on day 9 in culture. A representative experiment is shown in which the protective signal (the RFU [relative fluorescence units] difference between cultures treated with 100 nM KLS-13019 and 3 μM paclitaxel and those treated only with paclitaxel) was 4065 RFU. In contrast, the siRNA signal produced between the difference in fluorescence units from cultures treated with KLS-13019 plus paclitaxel from those treated with mNCX-1 siRNA and KLS-13019 and 3 μM paclitaxel was 3348 RFU. From these data, mNCX-1 siRNA produced a loss of 82 ± 3% of the protective signal. All experiments were conducted with this design, with only the protective agent (10 μM CBD or 100 nM KLS-13019) being different among the studies. In part B, a summary is

presented for the comparison of the siRNA-mediated decreases in protective activity produced by either 100 nM KLS-13019 or 10 μM CBD in the dark bars in replicate experiments for each protective agent. In the gray bars, the corresponding changes in neuritic mNCX-1 total spot area/10 fields for each experiment are shown. All bars represent the mean of 6 values ± the standard error. There were no significant differences among either the gray bars or among the dark bars in all 4 experiments indicating a similar % decrease in neuritic target mNCX-1 IR area and the % decrease in protective activity after mNCX-1 siRNA treatment.

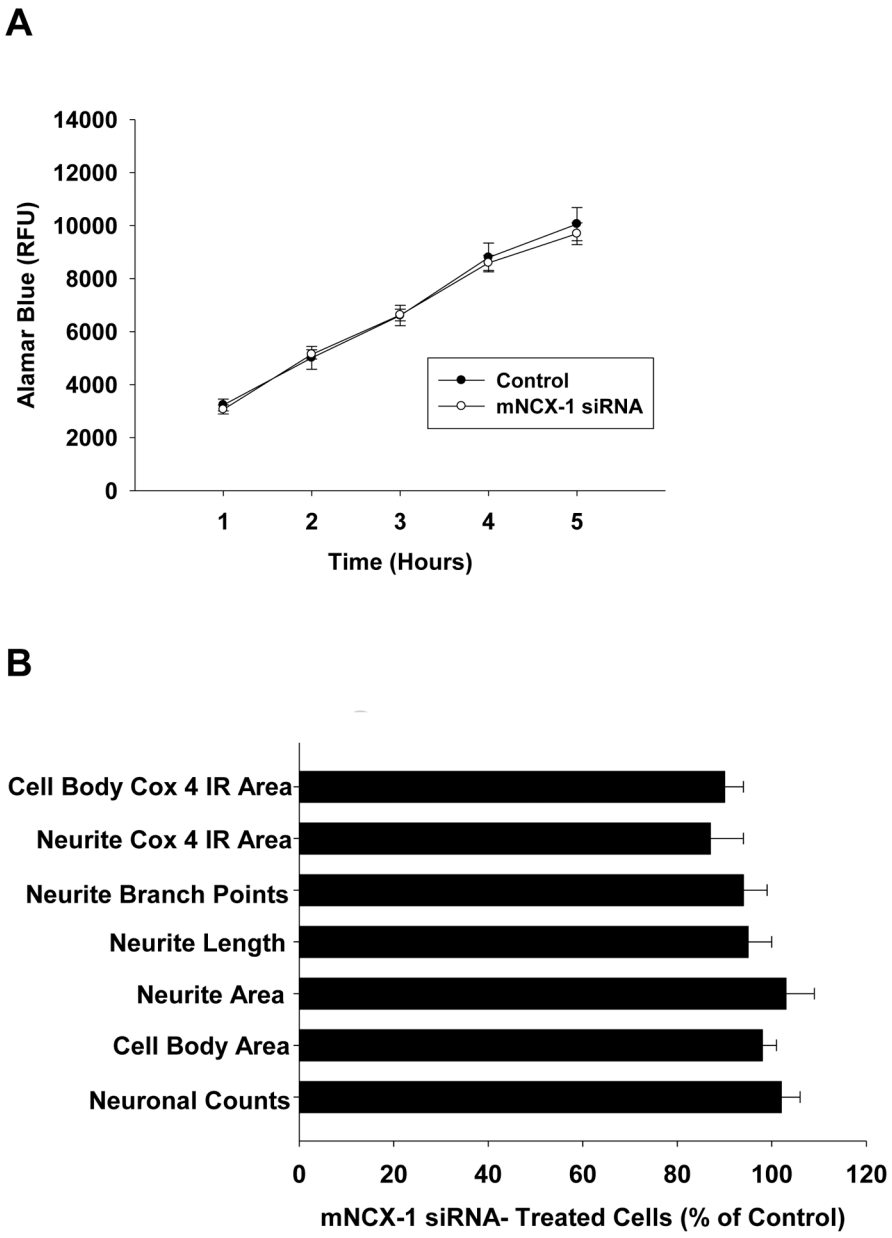

Fig. 9.

Multiple parameters of dorsal root ganglion cultures to demonstrate no significant toxicity after mNCX-1 siRNA treatment. In part A, a time course of Alamar Blue fluorescence response on day 9, which was 5 days after treatment with mNCX-1 siRNA. Control cultures (closed circles) are compared to response in mNCX-1 siRNA (open circles), indicating no significant difference between the groups at any time point from 1 to 5 hours (ANOVA). Each point is the mean of six determinations ± the standard error. In part B, high content image analyses of dorsal root ganglion were utilized to measure seven neuronal parameters. Control cultures were compared with cultures 5 days after treatment with mNCX-1 siRNA. Each value if the mean of 10 determinations from duplicate experiments ± the standard

error. No statistically significant differences were observed between the two groups for any of the neuronal parameters.